Adsorption of anionic and cationic dyes from aqueous solutions on fly ash-based porous geopolymer

Purbasari A.*, Ariyanti D. and Fitriani E.
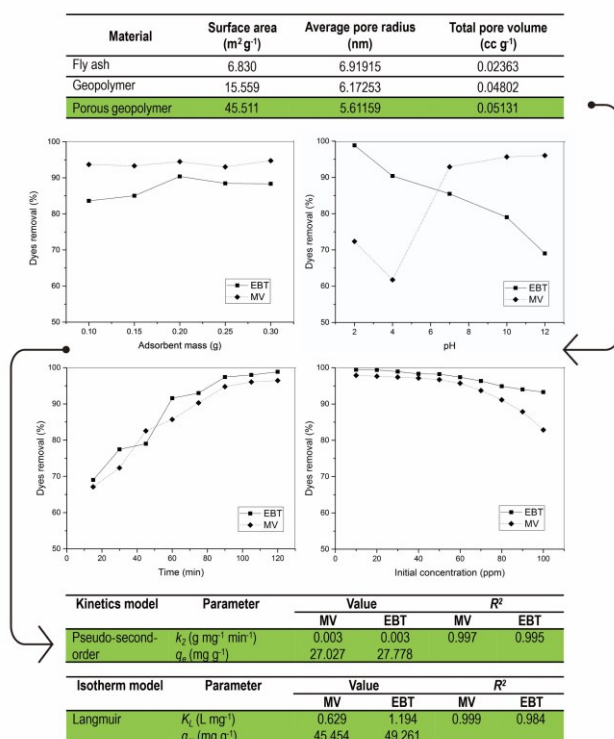
Department of Chemical Engineering, Faculty of Engineering, Universitas Diponegoro, Semarang, Indonesia

*to whom all correspondence should be addressed: e-mail: aprilina.purbasari@che.undip.ac.id

Graphical abstract

Abstract

Fly ash, solid waste from coal-fired power plant, had been utilized as raw material for porous geopolymer by alkaline activation and addition of hydrogen peroxide (H_2O_2) blowing agent. Porous geopolymer had higher surface area and total pore volume compared to fly ash and geopolymer without blowing agent, namely 45.511 $m^2\,g^{-1}$ and 0.05131 cc g^{-1}, respectively. Porous geopolymer was applied as adsorbent for anionic dyes Eriochrome Black T (EBT) and cationic dyes Methyl Violet (MV) from aqueous solutions. In this paper, factors affecting adsorption process such as adsorbent dosage, pH, time, and initial concentration were studied, in addition to adsorption kinetics and isotherm studies. Adsorbent dosage, time, and initial concentration factors had the same effect on the adsorption process for both EBT and MV dyes. The optimum removal efficiency was obtained at adsorbent dosage of 2 g L^{-1} and adsorption time of 90 minutes. The increase of the initial concentration of dyes would decrease the removal efficiency. For pH factor, adsorption of EBT dyes was better at pH of 2, while adsorption of MV dyes was better at pH of 10. Both adsorption of EBT and MV dyes by porous geopolymer followed pseudo-second-order kinetics model and Langmuir isotherm model with maximum adsorption capacity of 49.261 and 45.454 mg g^{-1}, respectively.

Keywords: Adsorption, fly ash, Eriochrome Black T, Methyl Violet, porous geopolymer

1. Introduction

Waste water containing dyes apart from causing aesthetic problems also causes health problems for living organisms. Dyes can act as allergic, mutagenic, carcinogenic, and toxic agents (Berradi *et al*. 2019; Lellis *et al*. 2019). In general, dyes can be classified as cationic, anionic, and nonionic dyes. Cationic dyes include azo basic, anthraquinone disperse, reactive dyes and are widely used in acrylic, nylon, silk, and wool dyeing. Anionic dyes include acid, direct, reactive dyes and are used in modified acrylic, polyamide, and polypropylene fibers dyeing; whereas nonionic dyes include disperse dyes for cellulose acetate, nylon, polyester, and acrylic fibers dyeing (Saini. 2017; Salleh *et al*. 2011).

The removal of dye pollutants in waste water can be done by physical, chemical, and biological methods. The physical methods consist of adsorption, filtration (microfiltration, nanofiltration, ultrafiltration, reverse osmosis), and irradiation. Meanwhile, examples of chemical methods are coagulation-flocculation, electrochemical treatment, oxidation, and photochemical treatment. For biological methods, there are aerobic and anaerobic treatments. Among those methods, adsorption is widely used because the process is simple, flexible, and effective with low cost (Kushwaha *et al*. 2013; Gita *et al*. 2017; Gherbia *et al*. 2019; Dutta *et al*. 2021). The common adsorbents for dyes removal are activated carbon, zeolite, and fly ash. Application of activated carbon from bamboo as adsorbent for wastewater from textile industry had showed efficiency of 91.84% (Salleh *et al*. 2011). Meanwhile, application of zeolite and fly ash adsorbents on textile wastewater had

showed efficiency of 90% and 40-90%, respectively (Hammood et al. 2021; Saini, 2017).

Geopolymer, inorganic polymer consisting of Si-O-Al bonds, has potential to be used as adsorbent for dyes removal due to its porous three dimensional structure (Siyal *et al*. 2018; Luukkonen *et al*. 2019). Like zeolite, geopolymer can be synthesized from fly ash which is solid waste from coal-fired power plant with alkaline activator. Alkaline activation of fly ash to form geopolymer takes place at temperature below 100 °C (Mehta and Siddique, 2016; Samadhi *et al*. 2017). The preparation of geopolymer is simpler than zeolite so that the use of geopolymer as dyes adsorbent deserves to be studied further. To improve the performance of geopolymer as adsorbent, blowing agents such as aluminum powder, silicon powder, hydrogen peroxide (H_2O_2), and sodium hypochlorite (NaOCl) can be added to the preparation of geopolymer. The blowing agents will form hydrogen (H_2) or oxygen (O_2) gases in geopolymer slurry so that porosity can increase which results in increase of geopolymer surface area (Barbosa *et al*. 2018; Bai and Colombo, 2018).

In this research, porous geopolymer was prepared from alkaline activation of fly ash with addition of H_2O_2 as blowing agent. Porous geopolymer was applied as adsorbent for dyes removal, namely cationic dyes Methyl Violet (MV) and anionic dyes Eriochrome Black T (EBT) from aqueous solutions. Factors affecting adsorption process like adsorbent dosage, pH, time, and initial concentration were studied. Furthermore, adsorption kinetics and isotherm studies were also conducted.

2. Materials and methods

2.1. Preparation and characterization of geopolymer and porous geopolymer

Materials used in this research were fly ash, sodium hydroxide (NaOH) flakes (98%), sodium silicate (Na-silicate) solution (35%), H_2O_2 solution (30%), nitric acid (HNO$_3$) solution (65%), MV and EBT dyes. Fly ash obtained from power plant in East Java, Indonesia had oxides composition as shown in Table 1 based on X-ray fluorescence (XRF) analysis. Fly ash was sieved with 100 mesh standard sieve before used.

Geopolymer was prepared by mixing of fly ash and alkaline activator with mass ratio of 2.5:1 in planetary mixer. The mixture was stirred at low speed for 10 minutes. Alkaline activator consisted of 10 N NaOH solution and Na-silicate solution with mass ratio of 1:1. For porous geopolymer, H_2O_2 as blowing agent was added to the mixture as much as 1 %-mass and stirred for 2 minutes. Geopolymer and porous geopolymer pastes were each casted in 5 cm x 5 cm x 5 cm molds. After 24 hours, geopolymer and porous geopolymer were removed from molds and heated in oven at 60 °C for 6 hours. Geopolymer and porous geopolymer then were crushed and characterized.

Characterization of fly ash, geopolymer, and porous geopolymer comprised Brunauer-Emmett-Teller (BET) surface area and pores size analysis using Nova 1200e Quantachrome instrument and scanning electron microscope (SEM) analysis using JEOL JSM 6510 LA instrument.

Table 1. Oxides composition of fly ash

Oxides	%-mass
Silicon dioxide (SiO_2)	32.452
Aluminium oxide (Al_2O_3)	16.453
Ferric oxide (Fe_2O_3)	23.782
Calcium oxide (CaO)	19.307
Magnesium oxide (MgO)	2.564
Potassium oxide (K_2O)	1.760
Phosphorus pentoxide (P_2O_5)	0.280
Sulfur trioxide (SO_3)	0.828
Titanium dioxide (TiO_2)	1.732
Vanadium oxide (V_2O_5)	0.124
Chromium oxide (Cr_2O_3)	0.069
Manganese oxide (MnO)	0.274
Nickel oxide (NiO)	0.029
Cupric oxide (CuO)	0.031
Zinc oxide (ZnO)	0.028
Rubidium oxide (Rb_2O)	0.018
Strontium oxide (SrO)	0.215
Zirconium dioxide (ZrO_2)	0.054

2.2. Adsorption process of dyes

Porous geopolymer was used as adsorbent of MV and EBT dyes. Adsorption was performed in batch process with 100 mL dyes solution at various adsorbent mass, pH, time, and initial concentration of dyes as shown in Table 2 at room temperature with stirring rate of 200 rpm. Concentration of dyes solution was measured using Thermo Scientific Genesys 10S UV-Vis spectrophotometer. Dyes removal efficiency (%) can be calculated with the equation:

$$Dyes\,removal\,efficiency\,(\%) = \frac{C_0 - C_e}{C_0}\,x100 \qquad (1)$$

C_0 is the initial dyes concentration (mg L^{-1}) and C_e is the dyes concentration at equilibrium (mg L^{-1}).

Table 2. Factors in adsorption process of dyes by porous geopolymer

Factor	Values
Adsorbent mass (g)	0.1, 0.15, 0.2, 0.25, 0.3
pH	2, 4, 7, 10, 12
Time (minutes)	15, 30, 45, 60, 75, 90, 105, 120
Initial concentration of dyes (mg L^{-1})	10, 20, 30, 40, 50, 60, 70, 80, 90, 100

2.3. Adsorption kinetics and isotherm studies

Adsorption kinetics studies in this research were conducted using pseudo-first-order, pseudo-second-order, and Elovich models which can be stated by these equations:

$$\ln(q_e - q_t) = lnq_e - k_1 t \qquad (2)$$

$$\frac{t}{q_t} = \frac{1}{k_2 q_e^2} + \frac{t}{q_e} \qquad (3)$$

$$q_t = \frac{1}{\beta}ln\alpha\beta + \frac{1}{\beta}lnt \qquad (4)$$

where q_t is the adsorption capacity at time t (mg g^{-1}) and q_e is the adsorption capacity at equilibrium (mg g^{-1}). Calculation of adsorption capacity can use this equation:

$$q = \frac{(C_0 - C_e)V}{W} \qquad (5)$$

where V is volume of dyes solution (L) and W is mass of porous geopolymer adsorbent (g) (Benjelloun *et al.*, 2021; Nizam *et al.*, 2021).

Moreover, adsorption isotherm studies were carried out using Langmuir, Freundlich, and Temkin models. Each of these models can be expressed by following equations:

$$q_e = \frac{q_m K_L C_e}{1 + K_L C_e} \qquad (6)$$

$$q_e = K_F C_e^{1/n} \qquad (7)$$

$$q_e = \frac{RT}{b} \ln(K_T C_e) \qquad (8)$$

where q_m is the maximum adsorption capacity (mg g^{-1}) (Al-Ghouti and Al-Absi, 2020; Wang and Guo, 2020).

3. Results and discussion

3.1. Characteristics of fly ash, geopolymer, and porous geopolymer

Physical properties of fly ash, geopolymer, and porous geopolymer comprising surface area, average radius, and total pore volume are shown in Table 3. Fly ash, geopolymer, and porous geopolymer can be classified as mesoporous materials because they contain pores with a width of 2-50 nm (ALOthman, 2012). Alkaline activation of fly ash into geopolymer can increase surface area and total pore volume of fly ash. Furthermore, the addition of H$_2$O$_2$ blowing agent in geopolymer formation can increase surface area and total pore volume of geopolymer. These physical properties support the application of porous geopolymer as adsorbent.

Table 3. Physical properties of fly ash, geopolymer, and porous geopolymer

Material	Surface area (m^2 g^{-1})	Average pore radius (nm)	Total pore volume (cc g^{-1})
Fly ash	6.830	6.91915	0.02363
Geopolymer	15.559	6.17253	0.04802
Porous geopolymer	45.511	5.61159	0.05131

The nitrogen adsorption-desorption isotherms of fly ash, geopolymer, and porous geopolymer are shown in Figure 1. These figures can indicate structural characterization of materials according to the International Union of Pure and Applied Chemistry (IUPAC) classification. Fly ash, geopolymer, and porous geopolymer can be classified as mesoporous materials because they have a hysteresis loop which indicates type IV isotherm. Type IV nitrogen adsorption-desorption isotherms are given from mesoporous materials that have a hysteresis loop exhibiting monolayer-multilayer physical adsorption and capillary condensation. The type of hysteresis loops for fly ash is H3 type from slit-shaped pores, while the type of hysteresis loops for geopolymer and porous geopolymer are H2 type from ink-bottle-shaped pores (ALOthman, 2012; Yuan *et al.*, 2019; Purbasari *et al.*, 2021).
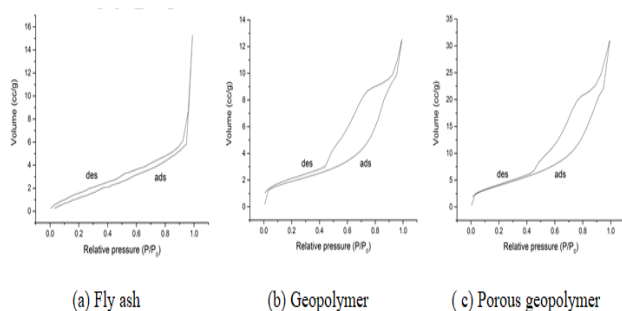
SEM micrographs with 1000x magnification for fly ash, geopolymer, and porous geopolymer are shown in Figure 2. The differences between these three materials could be seen in Figure 2 by naked eyes. Fly ash has spherical structure while geopolymer and porous geopolymer are amorphous due to the alkaline activation of fly ash (Kisku *et al.*, 2015; Purbasari *et al.*, 2018; El Alouani *et al.*, 2019). The space between molecules is increasing with the order of fly ash < geopolymer < porous geopolymer which is in accordance with the results of BET surface area and pores size analysis.
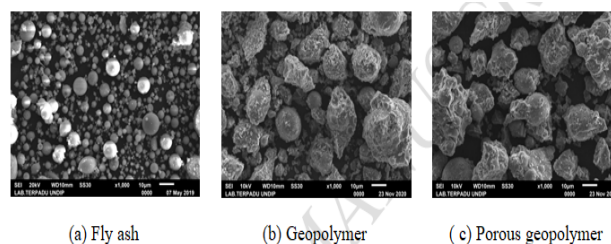
(a) Fly ash   (b) Geopolymer   (c) Porous geopolymer

Figure 2. Scanning electron micrographs of fly ash, geopolymer, and porous geopolymer

3.2. Adsorption of dyes using porous geopolymer

The obtained porous geopolymer was applied as adsorbent for MV and EBT dyes. The effect of adsorbent dosage on the dyes removal efficiency was studied using 100 mL dyes solution with concentration of 50 mg L^{-1} and pH of 7 for 2 hours. Figure 3 shows the usage of 0.2 g adsorbent give the optimum removal efficiencies for both MV and EBT dyes. Therefore, 0.2 g porous geopolymer was used in the next

(a) Fly ash   (b) Geopolymer   (c) Porous geopolymer

Figure 1. Nitrogen adsorption-desorption isotherms of fly ash, geopolymer, and porous geopolymer

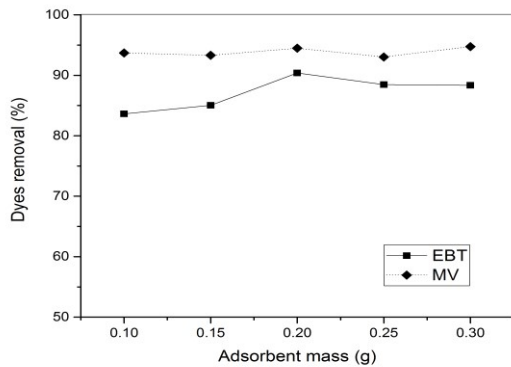adsorption process with variation of pH, time, and initial concentration.

Figure 3. The effect of adsorbent mass on the dyes removal efficiency

The effect of pH on the dyes removal efficiency can be observed from Figure 4. In this adsorption process, 100 mL dyes solution with concentration of 50 mg L^{-1} was adsorbed by 0.2 g porous geopolymer for 2 hours. The removal efficiency of MV dyes tends to increase up to pH of 10 and after that the removal efficiency slightly increases. Different result is shown by EBT dyes. The removal efficiency of EBT dyes tends to increase with the decrease of pH. The highest removal efficiency of EBT dyes is obtained at pH of 2. In high pH or basic solution, adsorbent surface becomes negatively charged from hydroxyl (OH^{-}) ions so that cationic dyes (MV) can be adsorbed easily on adsorbent surface. Meanwhile, low pH or acidic solution causes adsorbent surface to be positively charged from hydrogen (H^{+}) ions and is able to adsorb anionic dyes (EBT) (Salleh *et al*., 2011; Kushwaha *et al*., 2013).
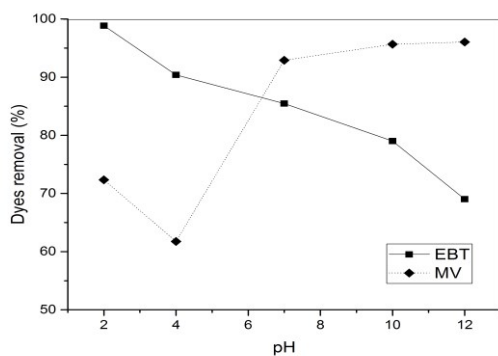

Figure 4. The effect of pH on the dyes removal efficiency

Figure 5 represents the effect of time on dyes adsorption by porous geopolymer. The dyes removal efficiency was observed using 100 mL dyes solution with concentration of 50 mg L^{-1} and adsorbent mass of 0.2 g for 2 hours with an interval of 15 minutes. Adsorption of MV dyes was done at pH of 10, while adsorption of EBT dyes was done at pH of 2. The dyes removal efficiencies for both MV and EBT dyes increase with the increase of time and reach equilibrium after 90 minutes. At the initial stage of adsorption process, there are still many available active sites on adsorbent surface so that the rate of dyes removal is high. At equilibrium stage, the rate of dyes removal becomes slower due to fewer active sites are available on adsorbent
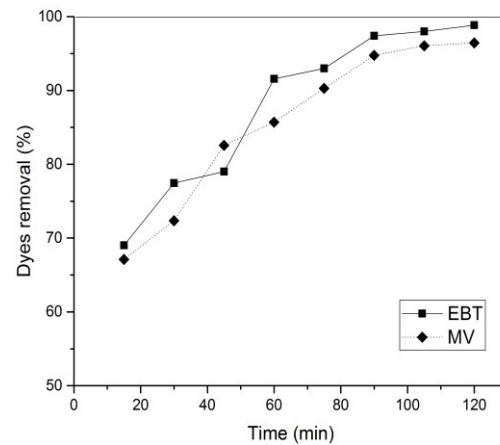
surface (Huang *et al*., 2017; Fernandes *et al*., 2020). The obtained data were then used for kinetics studies.

Figure 5. The effect of time on the dyes removal efficiency

Furthermore, the effect of initial concentration on dyes removal efficiency was studied using 100 mL dyes solution with 0.2 g adsorbent for 2 hours. Adsorption of MV dyes was carried out at pH of 10, while adsorption of EBT dyes was carried out at pH of 2. The obtained data were also used for isotherm studies. Figure 6 shows that the higher initial concentration of dyes solution, the lower dyes removal efficiency for both MV and EBT dyes. At low initial concentration, the number of active sites on the porous geopolymer surface can accommodate dyes adsorption process. However, the active sites on the porous geopolymer surface become insufficient to adsorb dyes at high initial concentration (Huang *et al*., 2017; Fernandes *et al*., 2020).
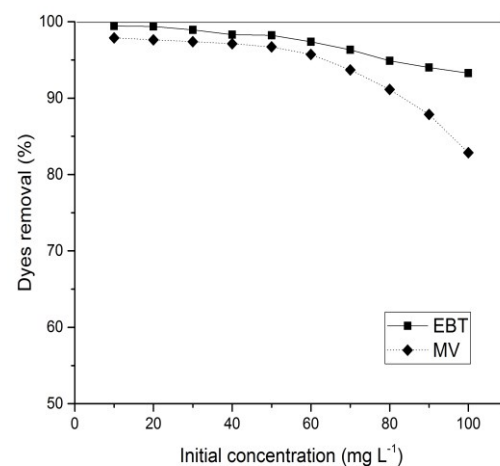

Figure 6. The effect of initial concentration on the dyes removal efficiency

3.3. Kinetics studies on dyes adsorption using porous geopolymer

Kinetics studies on MV and EBT adsorption by porous geopolymer were conducted using pseudo-first-order kinetics model, pseudo-second-order kinetics model, and Elovich kinetics model. In pseudo-first-order kinetics model, adsorption process is considered to be controlled by diffusion. Kinetics parameters for pseudo-first-order

model can be obtained by plotting linear equation (2), i.e. $ln(q_e - q_t)$ versus t. As for pseudo-second-order kinetics model, adsorption process is considered to be controlled by chemical adsorption. Kinetics parameters for pseudo-second-order model can be obtained by plotting linear equation (3), i.e. $\frac{t}{q_t}$ versus t. Meanwhile, in Elovich kinetics model, adsorption process is considered to be controlled by chemical adsorption on heterogeneous surface and kinetics parameters for Elovich model can be obtained by

plotting linear equation (4), i.e. q_t versus $ln\ t$ (Benjelloun *et al.*, 2021; Nizam *et al.*, 2021).

Table 4 shows kinetics parameters and correlation coefficients (R^2) for each kinetics model. Pseudo-second-order kinetics model has highest R^2 (close to 1) for both MV and EBT adsorption. This result indicates that adsorption of cationic and anionic dyes by porous geopolymer follows pseudo-second-order kinetics model or is controlled by chemical adsorption.

Table 4. Kinetics parameters and correlation coefficients for MV and EBT adsorption by porous geopolymer

Kinetics model	Parameter	Value		R^2	
		MV	EBT	MV	EBT
Pseudo-first- order	k_1 (min^{-1})	0.045	0.041	0.895	0.936
	q_e (mg g^{-1})	24.264	20.086		
Pseudo-second-order	k_2 (g mg^{-1} min^{-1})	0.003	0.003	0.997	0.995
	q_e (mg g^{-1})	27.027	27.778		
Elovich	α (mg g^{-1} min^{-1})	17.041	19.145	0.974	0.949
	β (g mg^{-1})	0.257	0.255		

Note: MV: Methyl Violet; EBT: Eriochrome Black T; k_1: pseudo-first-order rate constant; k_2: pseudo-second-order rate constant; q_e: adsorption capacity at equilibrium; α: initial adsorption rate constant; β: Elovich constant.

Table 5. Isotherm parameters and correlation coefficients for MV and EBT adsorption by porous geopolymer

Isotherm model	Parameter	Value		R^2	
		MV	EBT	MV	EBT
Langmuir	K_L (L mg^{-1})	0.629	1.194	0.999	0.984
	q_m (mg g^{-1})	45.454	49.261		
Freundlich	K_F (mg g^{-1} (L mg^{-1})$^{1/n}$)	14.825	22.182	0.899	0.972
	$1/n$	0.463	0.432		
Temkin	K_T (L g^{-1})	7.780	22.713	0.987	0.972
	b (J mol^{-1})	279.462	293.159		

Note: MV: Methyl Violet; EBT: Eriochrome Black T; K_L: Langmuir isotherm constant; q_m: maximum adsorption capacity; K_F: Freundlich isotherm constant; $1/n$: adsorption intensity; K_T: Temkin isotherm constant; b: Temkin constant related to the heat of sorption.

3.4. Isotherm studies on dyes adsorption using porous geopolymer

Isotherm studies to understand interaction between dyes adsorbate and porous geopolymer adsorbent were carried out using Langmuir isotherm model, Freundlich isotherm model, and Temkin isotherm model. Langmuir isotherm model describes that adsorbent surface is homogeneous so that there is monolayer adsorbate on the adsorbent surface, while Freundlich isotherm model describes that adsorbent surface is heterogeneous that has different adsorption abilities. Furthermore, Temkin isotherm model describes that there is uniform distribution of binding energies at adsorbent surface (Al-Ghouti and Al-Absi, 2020; Wang and Guo, 2020).

Isotherm parameters for Langmuir isotherm model, Freundlich isotherm model, and Temkin isotherm model can be obtained by plotting linear equation (6-8), namely C_e/q_e versus C_e, $log\ q_e$ versus $log\ C_e$, and q_e versus $ln\ C_e$, respectively. Isotherm parameters and R^2 for each isotherm model are presented on Table 5. Based on R^2, adsorption of MV and EBT by porous geopolymer tends to follow Langmuir isotherm model. Thus, there is only one

layer of dyes adsorbate formed on surface of porous geopolymer adsorbent.

The maximum adsorption capacity (q_m) of porous geopolymer for MV and EBT are 45.454 mg g^{-1} and 49.261 mg g^{-1}, respectively. For MV adsorption, this value is higher compared to zeolite and activated carbon/Fe$_3$O$_4$ magnetic nanocomposite adsorbents, namely 19.6 mg g^{-1} and 35.31 mg g^{-1}, respectively (Bertolini *et al.*, 2013; Foroutan *et al.*, 2021). Likewise for EBT adsorption, this value is higher compared to MnO$_2$-coated zeolite and NiFe$_2$O$_4$ magnetic nanoparticle adsorbents, namely 12.35 mg g^{-1} and 47.0 mg g^{-1}, respectively (Aguila and Ligaray, 2015; Moeinpour *et al.*, 2014).

Adsorption of cationic and anionic dyes by porous geopolymer that follows Langmuir isotherm model can be classified as favorable, unfavorable, linear, or irreversible adsorption from dimensionless separation factor (R_L):

$$R_L = \frac{1}{1 + K_L C_0} \tag{9}$$

which K_L is Langmuir constant and C_0 is initial concentration. The R_L value in the range of 0-1 indicates

favorable adsorption, $R_L > 1$ indicates unfavorable adsorption, $R_L = 1$ indicates linear adsorption, and $R_L = 0$ indicates irreversible adsorption (Amin *et al*., 2015). Adsorption of MV by porous geopolymer with initial concentration of 10-100 mg L^{-1} has R_L values of 0.137-0.016 and adsorption of EBT by porous geopolymer with initial concentration of 10-100 mg L^{-1} has R_L values of 0.077-0.008. These results indicate that adsorption of cationic and anionic dyes by porous geopolymer is favorable adsorption.

4. Conclusion

Porous geopolymer had been prepared from alkali activation of fly ash with addition of H_2O_2 blowing agent. Porous geopolymer with surface area of 45.511 m^2 g^{-1} and total pore volume of 0.05131 cc g^{-1} was then applied as adsorbent for cationic dyes MV and anionic dyes EBT from aqueous solutions. Factors affecting adsorption process had been studied and the results showed that optimum adsorbent dosage was 2 g L^{-1}, optimum adsorption time was 90 minutes, and dyes removal efficiencies decreased with increasing initial concentration. Meanwhile, optimum pH for MV dyes adsorption was 10 and for EBT dyes adsorption was 2. Adsorption of MV and EBT dyes by porous geopolymer followed pseudo-second-order kinetics model and Langmuir isotherm model. Maximum adsorption capacities of porous geopolymer on MV and EBT dyes were 45.454 mg g^{-1} and 49.261 mg g^{-1}, respectively.

References

Aguila D.M.M. and Ligaray M.V. (2015). Adsorption of Eriochrome Black T on MnO-coated zeolite, *International Journal of Environmental Science and Development,* **6**(11), 824–827.

Al-Ghouti M.A. and Al-Absi R.S. (2020). Mechanistic understanding of the adsorption and thermodynamic aspects of cationic Methylene Blue dye onto cellulosic olive stones biomass from wastewater, *Scientific Reports*, **10**, 15928.

ALOthman Z.A. (2012). A review: Fundamental aspects of silicate mesoporous materials, *Materials*, **5**, 2874–2902.

Amin M.T., Alazba A.A. and Shafiq M. (2015), Adsorptive removal of Reactive Black 5 from wastewater using bentonite clay: Isotherms, kinetics and thermodynamics, *Sustainability*, **7**, 15302–15318.

Bai C. and Colombo P. (2018). Processing, properties and applications of highly porous geopolymers: A review, *Ceramics International*, **44**(14), 16103–16118.

Barbosa T.R., Foletto E.L., Dotto G.L. and Jahn S.L. (2018). Preparation of mesoporous geopolymer using metakaolin and rice husk ash as synthesis precursors and its use as potential adsorbent to remove organic dye from aqueous solutions, *Ceramics International*, **44**(1), 416–423.

Benjelloun M., Miyah Y., Evrendilek G.A., Zerrouq F. and Lairini S. (2021). Recent advances in adsorption kinetic models: Their application to dye types, *Arabian Journal of Chemistry*, **14**(4), 103031.

Berradi M., Hsissou R., Khudhair M., Assouag M., Cherkaoui O., El Bachiri A. and El Harfi A. (2019). Textile finishing dyes and their impact on aquatic environs, *Heliyon*, **5**(11), e02711.

Bertolini T.C.R., Izidoro J.C., Magdalena C.P. and Fungaro D.A. (2013). Adsorption of Crystal Violet dye from aqueous solution onto zeolites from coal fly and bottom ashes, *Orbital: The Electronic Journal of Chemistry*, **5**(3), 179–191.

Dutta S., Gupta B., Srivastava S.K. and Gupta A.K. (2021). Recent advances on the removal of dyes from wastewater using various adsorbents: A critical review, *Materials Advances*, **2**, 4497–4531.

El Alouani M., Alehyen S., El Achouri M. and Taibi M. (2019). Comparative studies on removal of textile dye onto geopolymeric adsorbents, *EnvironmentAsia*, **12**(1), 143–153.

Fernandes J.V., Rodrigues A.M., Menezes R.R. and Neves G.A. (2020), Adsorption of anionic dye on the acid-functionalized bentonite, *Materials*, **13**, 3600.

Foroutan R., Peighambardoust S.J., Peighambardoust S.H., Pateiro M. and Lorenzo J.M. (2021). Adsorption of Crystal Violet dye using activated carbon of lemon wood and activated carbon/Fe$_3$O$_4$ magnetic nanocomposite from aqueous solutions: A kinetic, equilibrium and thermodynamic study, *Molecules*, **26**, 2241.

Gherbia A., Chergui A., Yeddou A.R., Selatnia Ammar S. and Boubekeur N. (2019). Removal of methylene blue using activated carbon prepared from date stones activated with NaOH, *Global NEST Journal*, **21**(3), 374–380.

Gita S., Hussan A. and Choudhury T.G. (2017). Impact of textile dyes waste on aquatic environments and its treatment, *Environment & Ecology*, **35**(3C), 2349–2353.

Hammood Z.A., Chyad T.F. and Al-Saedi R. (2021). Adsorption performance of dyes over zeolite for textile wastewater treatment, *Ecological Chemistry and Engineering S*, **28**(3), 329–337.

Huang Z., Li Y., Chen W., Shi J., Zhang N., Wang X., Li Z., Gao L. and Zhang, Y. (2017). Modified bentonite adsorption of organic pollutants of dye wastewater, *Materials Chemistry and Physics*, **202**, 266–276.

Kisku G.C., Markandeya M., Shukla S.P., Singh D.S. and Murthy R.C. (2015). Characterization and adsorptive capacity of coal fly ash from aqueous solutions of Disperse Blue and Disperse Orange dyes, *Environmental Earth Sciences*, **74**, 1125–1135.

Kushwaha S., Soni H., Ageetha V. and Padmaja P. (2013). An insight into the production, characterization, and mechanisms of action of low-cost adsorbents for removal of organics from aqueous solution, *Critical Reviews in Environmental Science and Technology*, **43**(5), 443–549.

Lellis B., Fávaro-Polonio C.Z., Pamphile J.A. and Polonio J.C. (2019). Effects of textile dyes on health and the environment and bioremediation potential of living organisms, *Biotechnology Research and Innovation*, **3**(2), 275–290.

Luukkonen T., Heponiemi A., Runtti H., Pesonen J., Yliniemi J. and Lassi U. (2019). Application of alkali-activated materials for water and wastewater treatment: A review, *Reviews in Environmental Science and Bio/Technology*, **18**, 271–297.

Mehta A. and Siddique R. (2016). An overview of geopolymers derived from industrial by-products, *Construction and Building Materials*, **127**, 183–198.

Moeinpour F., Alimoradi A. and Kazemi M. (2014). Efficient removal of Eriochrome black-T from aqueous solution using NiFe$_2$O$_4$ magnetic nanoparticles, *Journal of Environmental Health Science & Engineering*, **12**, 112.

Nizam N.U.M., Hanafiah M.M., Mahmoudi E., Halim A.A. and Mohammad A.W. (2021). The removal of anionic and cationic dyes from an aqueous solution using biomass-based activated carbon, *Scientific Reports*, **11**, 8623.

Purbasari A., Ariyanti D., Sumardiono S., Masyaroh M. and Salsabila T.R. (2021). Physical properties and structural characteristics of alkali modified fly ash, *Journal of Physics: Conference Series*, **1912**, 012012.

Purbasari A., Samadhi T.W. and Bindar Y. (2018). The effect of alkaline activator types on strength and microstructural properties of geopolymer from co-combustion residuals of bamboo and kaolin, *Indonesian Journal of Chemistry*, **18**(3), 397–402.

Saini R.D. (2017). Textile organic dyes: Polluting effects and elimination methods from textile waste water, *International Journal of Chemical Engineering Research*, **9**(1), 121–136.

Salleh M.A.M., Mahmoud D.K., Karim W.A.W.A. and Idris, A. (2011). Cationic and anionic dye adsorption by agricultural solid wastes: A comprehensive review, *Desalination*, **280**, 1–13.

Samadhi T.W., Wulandari W., Prasetyo M.I., Fernando M.R., and Purbasari A. (2017). Synthesis of geopolymer from biomass-coal ash blends, *AIP Conference Proceedings*, **1887**, 020031.

Siyal A.A., Shamsuddin M.R., Khan M.I., Rabat N.E., Zulfiqar M., Man Z., Siame J. and Azizli K.A. (2018). A review on geopolymers as emerging materials for the adsorption of heavy metals and dyes, *Journal of Environmental Management*, **224**, 327–339.

Wang J. and Guo X. (2020). Adsorption isotherm models: Classification, physical meaning, application and solving method, *Chemosphere*, **258**, 127279.

Yuan N., Cai H., Liu T., Huang Q. and Zhang X. (2019). Adsorptive removal of methylene blue from aqueous solution using coal fly ash-derived mesoporous silica material, *Adsorption Science & Technology*, **37**(3–4), 333–348.